Unidirectional stratified flow through a non-rectangular channel

By ANDERS ENGQVIST[1] AND ANDREW McC. HOGG[2]

[1]Department of Systems Ecology, Stockholm University, SE-106 91 Stockholm, Sweden

[2]James Rennell Division, Southampton Oceanography Centre, European Way, Southampton SO14 3ZH, UK

A self-similar solution describing stratified flow through a non-rectangular channel is derived. The solution shown here is an extension of Wood's (1968) solution for stratified withdrawal through a rectangular channel. We consider a restricted set of geometries (where the bottom of the channel is constrained to be flat) and calculate the flow, assuming first multi-layer stratification, and second continuous stratification. In the case of two-layer flow we prove that the self-similar solution is the only possible solution. The analytical solutions are corroborated by three-dimensional numerical model simulations.

1. Introduction

The study of withdrawal of a stratified fluid from a stagnant reservoir has applications in geophysics (such as flow of ocean bottom water through gaps in mid-ocean ridges) as well as engineering (e.g. withdrawal from a reservoir) and flow of air through doors and windows. This problem was first considered by Wood (1968), who wrote a seminal paper in which the notion of hydraulic control was illustrated. Wood's (1968) self-similar solution demonstrated that for stratified withdrawal through a contracting channel with a rectangular cross-section, layers reduced their thickness by a factor of 2/3 between the stagnant reservoir and the centre of the contraction. At the centre of the contraction a point of hydraulic control is found, where the propagation of internal waves in the direction opposite to the flow is arrested. Benjamin (1981) investigated this type of flow in greater detail, proposing that the self-similar solution is the only one which is selected for flows drawn from a stagnant reservoir.

Laboratory experiments on unidirectional stratified flows have demonstrated the relevance of self-similar solutions to the flows observed. Armi & Williams (1993) showed a number of different cases where self-similar flows, bounded by either stationary fluid or a solid flat boundary, formed in a laboratory flume.

In principle, hydraulic solutions can be used to describe flow in a number of situations, such as deep overflows in the ocean, flow at the mouth of estuaries and flow within reservoirs. Application of the stratified withdrawal solutions are complicated by several factors, including the effect of mixing upon the flow, the rotation of the Earth, time dependence, the introduction of bottom topography and the possibility of sloping sidewalls to the channel. In this note we address the last point raised here, and argue that self-similar solutions are possible for a restricted set of geometries in which the sidewalls are sloping, but the bottom of the channel is flat. We adopt a simplified version of the geometry used by Dalziel (1992), so that the form of the
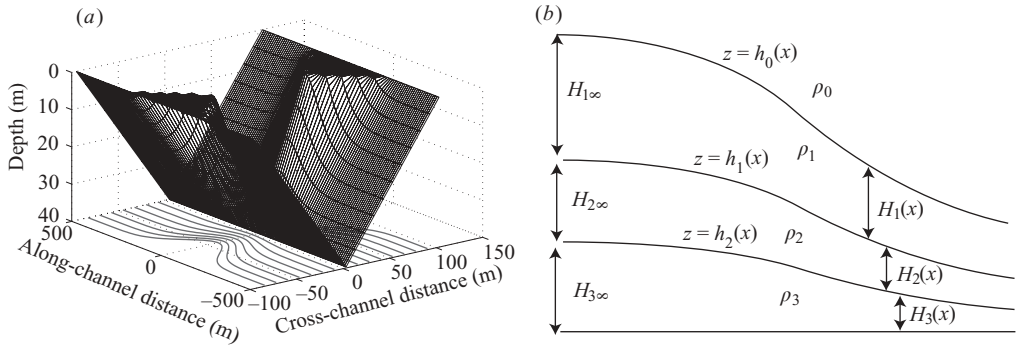
FIGURE 1. (*a*) Channel geometry for a triangular channel ($\beta = 1$); (*b*) layer numbering system for the example of three layers.

channel as a function of x does not change, but the width of the channel varies to form a contraction.

Two methods have previously been used for investigating these flows; we explore this problem using both techniques. First, we use the multi-layer formulation, following previous studies by Baines (1988) and Engqvist (1996). The multi-layer solution gives rise to some tedious algebra for large numbers of layers, but has the advantage that one can easily interpret the results, and pinpoint the virtual control points. In addition, by reducing the multi-layer solution to just two active layers we are able to show that the self-similar solution is the only solution. By invoking an induction-based proof we extend this to apply to an infinite number of layers. We also solve the problem with arbitrary continuous stable stratification in the upstream reservoir using the methodology of Killworth (1992) and Hogg & Killworth (2004). Here we find that self-similar solutions can also be found, and that the control condition at the topographic minimum of the channel is identical to the layered case.

2. Multi-layer solution

We seek a solution for uni-directional stratified flow through a flat-bottomed channel which has walls which may not be vertical. Start by writing the width as a function of the streamwise coordinate x and height z as

$$b(x, z) = b_0(x)z^{\beta}. \tag{2.1}$$

Here b_0 is the width of the channel at the top of the stagnant layer (which is horizontal), and β is the factor used by Dalziel (1992), where $\beta = 0$ corresponds to a rectangular channel, $\beta = 1$ to a triangular channel (see figure 1*a*) and if $\beta = \frac{1}{2}$ the channel is parabolic. Note that the difference between our formulation and that of Dalziel is that we have not allowed variations in the depth of the channel with x.

In the absence of viscosity energy is constant along streamlines; in other words

$$\tfrac{1}{2}u^2 + B = B_{\infty}, \tag{2.2}$$

where u is the horizontal velocity, and $B(x, z) = (p + \rho g z)/\rho_0$ is the Bernoulli function comprising pressure p, density ρ, constant reference density ρ_0 and acceleration due to gravity g. The upstream boundary is assumed to be an infinitely wide reservoir of known stratification, in which velocities are zero and the Bernoulli function is given by B_{∞}. Bounding our fluid above is a stagnant layer of constant density, and we

assume that at some point downstream of the contraction the channel once again becomes infinitely wide, with the same density of the overlying fluid.

Following Engqvist (1996) we divide the flow into a finite number of layers, where layer 0 is a stagnant upper layer of density ρ_0. Active layers are numbered from 1 to n starting from the uppermost layer. The layer thicknesses H_i and interface heights h_i are as illustrated in figure 1(b). The momentum equation for the ith layer is then

$$\rho_i u_i u_{i,x} = -g \sum_{j=1}^{i} \Delta\rho_j h_{j-1,x}, \tag{2.3}$$

where $\Delta\rho_j = \rho_j - \rho_{j-1}$ is positive. The continuity equation for each layer is simply

$$(u_i \overline{W_i} H_i)_{,x} = 0 \tag{2.4}$$

where the mean width $\overline{W_i}$ is defined below.

We define several additional quantities relating to the geometry of the flow. The mid-height of each layer is denoted

$$\overline{h_i} = \tfrac{1}{2}(h_{i-1} + h_i), \tag{2.5}$$

and we approximate the mean width of the layer using (2.1):

$$\overline{W_i}(x) = b_0(x)\overline{h_i}^{\beta}. \tag{2.6}$$

This approximation is only exact when the sides of the channel are straight (i.e. for β equal to 0 or 1). However, it tends towards an exact solution as the number of layers becomes large. The derivative of (2.6), after application of the chain rule, can be written as

$$\overline{W}_{i,x} = \frac{\overline{W_i} b_{0,x}}{b_0} + \frac{\beta \overline{W_i}}{\overline{h_i}}, \tag{2.7}$$

and substituted into the continuity equation (2.4) to give an expression for the x-derivative of velocity,

$$u_{i,x} = -\frac{u_i}{H_i} \left(\frac{H_i}{b_0} b_{0,x} + \frac{\beta H_i}{\overline{h_i}} \overline{h}_{i,x} + H_{i,x} \right) \tag{2.8}$$

which applies everywhere in the channel. Substituting $H_{i,x} = h_{i-1,x} - h_{i,x}$ and (2.5) gives the velocity derivative in terms of interface height derivatives,

$$u_{i,x} = -\frac{u_i}{H_i} \left(\frac{H_i}{b_0} b_{0,x} + \frac{\beta H_i}{2\overline{h_i}}(h_{i-1,x} + h_{i,x}) + h_{i-1,x} - h_{i,x} \right), \tag{2.9}$$

which we substitute into (2.3) to give

$$\frac{\rho_i u_i^2}{H_i} \left(\frac{H_i}{b_0} b_{0,x} + \frac{\beta H_i}{2\overline{h_i}}(h_{i-1,x} + h_{i,x}) + h_{i-1,x} - h_{i,x} \right) = -g \sum_{j=1}^{i} \Delta\rho_j h_{j-1,x}. \tag{2.10}$$

This equation shows that there is a relationship between each layer and the one above,

$$\frac{\rho_{i+1} u_{i+1}^2}{H_{i+1}} \left(\frac{H_{i+1}}{b_0} b_{0,x} + \frac{\beta H_{i+1}}{2\overline{h_{i+1}}}(h_{i,x} + h_{i+1,x}) + h_{i,x} - h_{i+1,x} \right)$$
$$= \frac{\rho_i u_i^2}{H_i} \left(\frac{H_i}{b_0} b_{0,x} + \frac{\beta H_i}{2\overline{h_i}}(h_{i-1,x} + h_{i,x}) + h_{i-1,x} - h_{i,x} \right) + g\Delta\rho_{i+1} h_{i,x}. \tag{2.11}$$

For illustrative purposes we simplify this situation slightly, by assuming that $\Delta\rho_i = \Delta\rho$ for all i (although it should be noted that in the analysis which follows, all results still hold if this assumption is relaxed). The layer Froude numbers f_i are defined as

$$f_i^2 = \frac{\rho_0 u_i^2}{g\Delta\rho H_i}$$

so that our equation can be written in matrix form as follows:

$$\begin{bmatrix} 1 - f_{1+}^2 & f_{1-}^2 & 0 \\ f_{1+}^2 & 1 - f_{1-}^2 - f_{2+}^2 & f_{2-}^2 \\ 0 & f_{2+}^2 & 1 - f_{2-}^2 - f_{3+}^2 \end{bmatrix} \begin{bmatrix} h_{0,x} \\ h_{1,x} \\ h_{2,x} \end{bmatrix} = \begin{bmatrix} f_1^2 H_1 \\ f_2^2 H_2 - f_1^2 H_1 \\ f_3^2 H_3 - f_2^2 H_2 \end{bmatrix} \frac{b_{0,x}}{b_0}, \quad (2.12)$$

where we have again simplified the situation by assuming only three layers, and defined

$$f_{i\pm}^2 = f_i^2 \left(1 \pm \frac{\beta H_i}{2\overline{h}_i} \right).$$

This matrix equation shows that at the centre of the contraction where $b_{0,x} = 0$, then either every interface height has zero gradient there, or else the determinant of the matrix on the left-hand side of this equation is zero. In the latter case the restriction on the matrix determinant yields a control condition similar to that derived by Baines (1988) for a rectangular channel which describes the transition from sub- to supercritical flow. In the first case the solution does not change criticality at the throat, so that for the upstream boundary condition used here, flow is subcritical everywhere.

This determinant equation can be used to give an exact solution if one is prepared to assume that the flow is self-similar. To demonstrate this we take the two-layer case, and write layer thicknesses in terms of their upstream value and a height reduction factor

$$H_i = \alpha_i(x) H_{i\infty}.$$

The upper streamline of each layer behaves according to (2.2), which allows us to find Froude numbers as a function of the Bernoulli function B. It is easy to verify that the Froude numbers are given by

$$f_1^2 = \frac{2}{\alpha_1 H_{1\infty}} (H_{1\infty}(1 - \alpha_1) + H_{2\infty}(1 - \alpha_2)), \quad (2.13)$$

$$f_2^2 = \frac{2}{\alpha_2 H_{2\infty}} (H_{1\infty}(1 - \alpha_1) + 2H_{2\infty}(1 - \alpha_2)). \quad (2.14)$$

Self-similarity means that each layer contracts by the same amount between the reservoir and any point x, or $\alpha_1 = \alpha_2 = \alpha$. The Froude numbers squared for a self-similar flow are then

$$f_{1\pm}^2 = \frac{2(H_{1\infty} + H_{2\infty})(1 - \alpha)}{H_{1\infty}\alpha} \left(1 \pm \frac{\beta H_{1\infty}}{H_{1\infty} + 2H_{2\infty}} \right),$$

$$f_{2\pm}^2 = \frac{2(H_{1\infty} + 2H_{2\infty})(1 - \alpha)}{H_{2\infty}\alpha} (1 \pm \beta).$$

By setting the determinant of the matrix on the left-hand side of (2.12) to zero, we recover

$$\alpha_{gc} = \frac{2 + 2\beta}{3 + 2\beta}, \tag{2.15}$$

which is the geometric control point, reducing to Wood's familiar $\frac{2}{3}$ in a straight-walled channel ($\beta = 0$), and which depends upon the channel shape but not the layer structure.

The second root,

$$\alpha_{vc} = 1 - \frac{H_{1\infty} H_{2\infty}}{2\beta H_{1\infty}(H_{1\infty} + H_{2\infty}) + 2H_{1\infty}^2 + 7H_{1\infty} H_{2\infty} + 4H_{2\infty}^2}, \tag{2.16}$$

is, in general, a virtual control point which occurs upstream of the contraction. As one increases the number of layers, another virtual control is created for each additional layer, with the value of α at the virtual controls tending to 1 as $n \to \infty$.

We have found that for two layers, the self-similar vertical height reduction at the geometrical control is α_{gc}. We will now prove that this holds for any number of layers using induction; in other words if it holds for n layers, it will still hold when a new $(n + 1)$th layer is inserted. The reservoir height of the top of the nth layer (that is, the bottom layer) is rescaled to be unity and a new layer is inserted beneath it with height h. Under this manipulation neither the geometric shape nor the flow parameters of the top $n - 1$ layers will be changed. In order to distinguish the Froude number of the nth layer before and after this manipulation, the former value is marked with a prime. Expanding (2.12) along the bottom row at the geometric control for the n-layer case then yields

$$D_{n-1}\left[1 - f_{(n-1)-}^2 - f_{n+}'^2\right] - f_{(n-1)+}^2 f_{(n-1)-}^2 = 0, \tag{2.17}$$

in which D_{n-1} denotes the $(n-1) \times (n-1)$ cofactor determinant with coinciding diagonal to (2.12).

After insertion of the $(n + 1)$th layer, the velocity of the nth layer is unchanged and thus $f_{n+}'^2 = (1 - h)f_n^2(1 + \beta)$ and $f_{n\pm}^2 = f_n^2(1 \pm \beta(1 - h)/(1 + h))$ hold. In analogy to the two-layer case, the Froude numbers as a function of the layer heights are

$$f_n^2 = \frac{2}{H_n}(H_0 + 1 - H_n - H_{n+1}) \tag{2.18}$$

and

$$f_{(n+1)+}^2 = \frac{2}{H_{n+1}}(H_0 + 1 - H_n - H_{n+1} + h - H_{n+1})(1 + \beta). \tag{2.19}$$

The introduced variable H_0 represents the resulting acceleration of the $n - 1$ layers above and may be expressed as $(1 - \alpha_{gc})\sum h_j$, with the summation taken over the top n interfaces. However, the exact appearance of this term turns out to be inconsequential, since the terms containing H_0 will eventually cancel. Expanding the bottom row as in (2.17) with the $(n + 1)$th layer inserted gives

$$\left(1 - f_{n-}^2 - f_{(n+1)+}^2\right)\left[D_{n-1}\left(1 - f_{n-1)-}^2 - f_{n+}^2\right) - f_{(n-1)+}^2 f_{(n-1)-}^2\right] - D_{n-1}f_{n+}^2 f_{n-}^2 = 0. \tag{2.20}$$

Subtracting and adding the terms containing $f_{n+}'^2$ and f_{n+}^2 respectively from and to (2.17) and substituting the resulting expression into the second term of (2.20) finally gives a relationship between the Froude numbers of the two bottommost layers:

$$f_{n+}^2 f_{n-}^2 + \left(1 - f_{n-}^2 - f_{(n+1)+}^2\right)f_n^2 h\left[1 - \beta\frac{1 - h}{1 + h}\right] = 0. \tag{2.21}$$

Inserting the Froude numbers evaluated with $H_{n+1} = \alpha h$ and $H_n = \alpha(1 - h)$ yields the solution $\alpha = \alpha_{gc}$, which proves by induction that the solution found is valid for an arbitrary number of layers.

3. Validity of the self-similar assumption

In the previous section we showed the existence of a self-similar solution for stratified flow through the channels considered. In keeping with previous work on this subject our approach was to assume that self-similarity applied; this approach was justified by Wood (1968) by referring to the two-layer solution in which the self-similar solution was the only one connecting the upstream and downstream conditions. We now extend this two-layer solution to channels with sloping sidewalls.

This could be achieved by first finding the location of the virtual control, solving (2.12) and then using the same equation to integrate the solution in either direction. More instructive, however, is to use the constant layer fluxes

$$Q_i = \sqrt{g\Delta\rho\overline{W_i}^2 H_i^3 f_i^2 / \rho_i},$$

to write a ratio which is constant for all x:

$$\frac{Q_1^2}{Q_2^2} = \frac{\rho_2}{\rho_1} \frac{f_1^2}{f_2^2} \frac{H_1^3}{H_2^3} \frac{\overline{W_1}^2}{\overline{W_2}^2}. \tag{3.1}$$

To demonstrate the point being made here we select the case where upstream layer heights are equal ($H_{1\infty} = H_{2\infty}$); the results are not sensitive to this assumption, but the algebra is simplified considerably. We then substitute (2.13) and (2.14) into (3.1) to give

$$\frac{Q_1^2}{Q_2^2} = \frac{\rho_2}{\rho_1} \frac{\alpha_1^2}{\alpha_2^2} \frac{(2 - \alpha_1 - \alpha_2)}{(3 - \alpha_1 - 2\alpha_2)} \left(\frac{2\alpha_2 + \alpha_1}{\alpha_2}\right)^{2\beta}. \tag{3.2}$$

In fact, when self-similarity is assumed ($\alpha_1 = \alpha_2$) this ratio is independent of x. We look for other plausible roots of this equation by evaluating this constant expression at the virtual control point:

$$3\alpha_1^2(2 - \alpha_1 - \alpha_2)(2\alpha_2 + \alpha_1)^{2\beta} = 2\alpha_2^2(3 - \alpha_1 - 2\alpha_2)(3\alpha_2)^{2\beta}. \tag{3.3}$$

One solution of this equation is $\alpha_1 = \alpha_2$; additional solutions depend upon the value of β. We show an example in figure 2 using $\beta = \frac{1}{2}$ (parabolic channel). Here we see that the solid line ($\alpha_1 = \alpha_2$) is the only root connecting the reservoir conditions at (1,1) to the virtual control, the geometric control and the downstream asymptotic solution where both layers become infinitely thin. In this case three other roots exist. Only one of these solutions is physically plausible (i.e. it exists in the range [0,1]); it is shown by the dashed line in figure 2, and intersects the self-similar solution at the virtual control.

Thus the nature of the the self-similar solution for the two-layer case is clear. Like Wood (1968), we are hesitant to tackle the algebra for more than two layers, but instead proceed to show that the self-similar solution can exist for this flow with arbitrary upstream stratification.
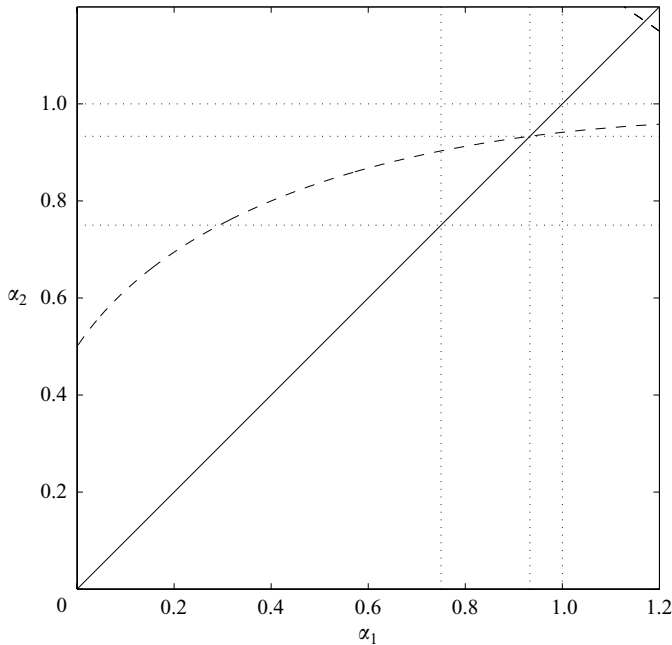
FIGURE 2. Physically plausible solutions of (3.3), with the self-similar solution shown by the solid line. The reservoir height of each layer is 1, and positions of virtual and geometric control are marked.

4. Continuously stratified solution

To calculate a solution for continuously stratified flow, the channel geometry in this case requires us to integrate the continuity equation across the channel:

$$\int_0^{b(x,z)} u_x \mathrm{d}y + \int_0^{b(x,z)} v_y \mathrm{d}y + \int_0^{b(x,z)} w_z \mathrm{d}y = 0, \tag{4.1}$$

which simply becomes

$$b u_x + \int_0^{v_w} \mathrm{d}v + b w_z = 0. \tag{4.2}$$

Here v_w is the velocity along the channel wall, which can be calculated from the other two components of velocity ($v_w = b_x u + b_z w$), so that

$$(bu)_x + (bw)_z = 0. \tag{4.3}$$

We now proceed by transforming from (x, z) coordinates to (X, η) coordinates where $x = X$ and η is the height of the streamline in the upstream reservoir. To do this, note that we can use the chain rule in combination with $x_\eta = 0$ and $x_X = 1$, leaving

$$\frac{\partial}{\partial X} \rightarrow \frac{\partial}{\partial x} + z_X \frac{\partial}{\partial z}, \quad \frac{\partial}{\partial \eta} \rightarrow z_\eta \frac{\partial}{\partial z}.$$

These are inverted and applied to (4.3) to give

$$(bu)_X - \frac{z_X}{z_\eta}(bu)_\eta + \frac{1}{z_\eta}(bw)_\eta = 0. \tag{4.4}$$

Note that vertical velocity is simply horizontal velocity multiplied by the streamline slope ($w = uz_X$), leaving simply

$$(buz_\eta)_X = 0. \tag{4.5}$$

This is the same form as for cases with vertical sidewalls (see (2.6) in Hogg & Killworth 2004).

We now assume that flow within the layer is self-similar, or in other words the height and energy of a streamline can be separated into X- and η-dependent parts:

$$z(X, \eta) = \alpha(X)\eta, \quad B(X, \eta) = \alpha(X)B_\infty(\eta), \tag{4.6a, b}$$

and thus write (2.2) and (4.5) respectively as

$$u = (2B_\infty(1 - \alpha))^{1/2}, \tag{4.7}$$

$$b_0(\alpha\eta)^\beta u\alpha = Q(\eta), \tag{4.8}$$

where we have included the width information from (2.1). These are combined to give

$$b_0\alpha^{(\beta+1)}(1 - \alpha)^{1/2} = \frac{Q(\eta)}{(2B_\infty)^{1/2}\,\eta^\beta}, \tag{4.9}$$

in which the left-hand side depends only upon X and the right-hand side only upon η. The control condition can be found by differentiation with respect to X:

$$\frac{1}{b_0}\frac{\mathrm{d}b_0}{\mathrm{d}X} = \frac{\mathrm{d}\alpha}{\mathrm{d}X}\left(\frac{(2\beta + 3)\alpha - 2(\beta + 1)}{2\alpha(1 - \alpha)}\right). \tag{4.10}$$

The geometrical control condition is then identical to that given by (2.15).

5. Numerical simulation results

For a rectangular channel the control condition gives $\alpha_{gc} = \frac{2}{3}$, and $\alpha_{gc} = \frac{3}{4}, \frac{4}{5}$ and $\frac{6}{7}$ correspond to channel cross-sections that are parabolic, triangular and hyperbolic respectively. Employing a three-dimensional numerical model MITgcm (Marshall *et al.* 1997), set up with boundary conditions according to Stenström (2003), these theoretical results may be tested. The numerical tests differ from the theory in two ways. First, while the theory is inviscid and non-diffusive, the model is not. In spite of the efforts made to reduce the diapycnal mixing it cannot be completely eliminated and acts to blur the isopycnals. Second, in the theory there is an infinite cross-section area ratio between the far upstream and the narrowest constriction. In the model this can only be achieved at the expense of computational effort in the same proportion. The compromise made is depicted in figures 1(*a*) and 3 in which effects of the non-hydrostatic approach control (see Zhu & Lawrence 1998) are visible together with aberrations from horizontal cross-sectional interfaces. Taken together these factors combine to produce significant uncertainty in the simulated values of α_{gc}. Figure 3 shows the modelled steady-state flow through a triangular channel, indicating the uncertainty involved in measuring α_{gc}. The comparison between theory and simulation is shown in table 1 for four different channels. In each case the model and theory agree within the estimated uncertainty. Unexpectedly, these uncertainties increase for small β-values. Even with the liberal allowances made when estimating these, the layer averages of the simulated α_{gc}-values provide corroborative evidence that the present theory applies.
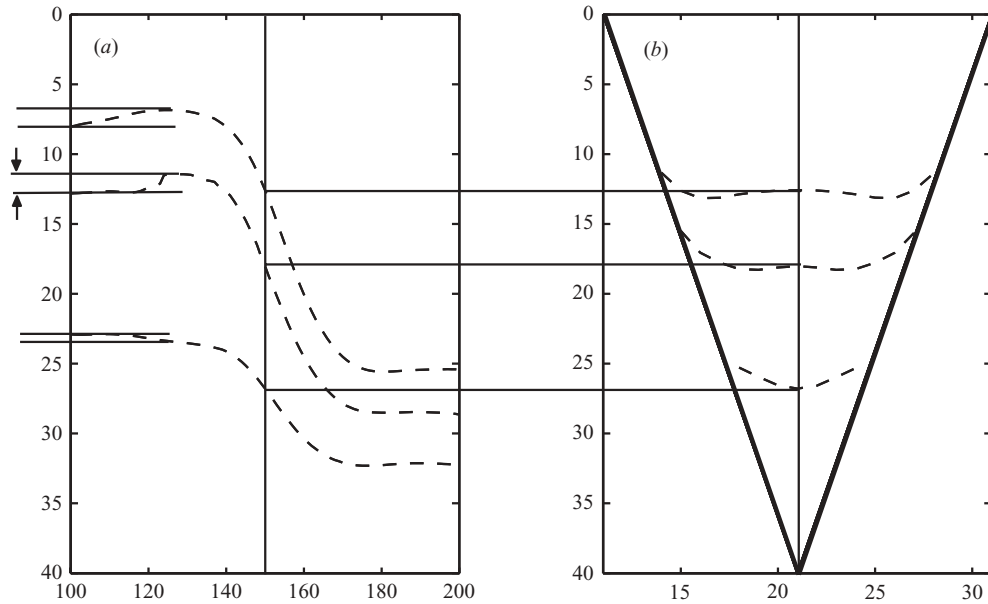
FIGURE 3. (a) Cissect through the mid-section, and (b) transect at the geometrical control for a three-layer simulation with $\beta = 1$ showing unfiltered raw data isopycnals, with equal density differences between adjacent layers. The uncertainties due to approach control and non-horizontal interfacial cross-section are apparent. The former is indicated for the mid-interface with a pair of arrows.

β	α_{gc} (model)	α_{gc} (theory)
0.0	0.74 ± 0.07	0.67
0.5	0.76 ± 0.05	0.75
1.0	0.82 ± 0.04	0.80
2.0	0.84 ± 0.03	0.86

TABLE 1. Average vertical height reduction of three active layers similar to figure 3 together with an estimated S.D. compared to the theoretically expected value.

6. Discussion

The inherent nature of the self-similar solutions is most clearly revealed by (3.2) in which the flow ratio between layers is proved to be constant throughout the domain, provided that $\alpha_1 = \alpha_2$. Combined with a cross-section geometry that also maintains the layer area ratio regardless of the vertical self-similar height reduction, a steady flow can be sustained throughout the channel. Both (3.2) and (4.9) reveal that the so-called Dalziel-geometry (1992) is the unique set of shapes for which this holds true by cancelling the α-factor in the former case and making the equation separable in the latter.

The α_{gc}-factor for controlled flow beneath a stagnant layer in (2.15) was derived earlier by Dalziel (1992), but for one-layer flow through a flat-bottom channel. This instance would thus have sufficed as a starting point for the induction-based proof in §3. The simplifying assumption made in §2 with an equal density difference between layers could be relaxed. The $f_i^{\,2}$-matrix would then also contain density quotients (r_i)

according to, for example equation (27) in Lane-Serff, Smeed & Postlethwaite (2000). Likewise the 'mid-height' approximation leading to (2.6) could possibly also be relaxed since in (2.8) the sole appearance of the $\overline{h_i}$-term is as a quotient between its derivative and itself. The pursuit of the algebra with $\overline{h_i}$ representing the exact average width entails considerably more complicated weight-coefficients than the 0.5-factors used here for $h_{i-1,x}$ and $h_{i,x}$ in (2.9) and does not seem to elucidate the physics more than the algebra is obscured.

It was pointed out by Wood (1968) that his solution for two-layer flow through a rectangular cross-section required no assumption of Boussinesq stratification. This also applies to the multi-layered solutions presented here. Arbitrarily strong gradients may thus be approximated by making the individual layers sufficiently thin.

The self-similar solutions presented here require a number of conditions, including a flat-bottomed channel, to be exact. Therefore, direct application to, for example, oceanographic flows is limited; however solutions such as these greatly enhance physical understanding of the mechanisms underpinning nonlinear stratified flows. In addition, they represent incremental progress towards more general hydraulic solutions. For example, Engqvist & Stenström (2004) discuss the possibility of expanding existing solutions to exchange flows, provided that there is only one homogeneous contra-flowing top layer.

REFERENCES

Armi, L. & Williams, R. 1993 The hydraulics of a stratified fluid flowing through a contraction. *J. Fluid Mech.* **251**, 355–375.

Baines, P. G. 1988 A general method for determining upstream effects instratified flow of finite depth over long two-dimensional obstacles. *J. Fluid Mech.* **188**, 1–22.

Benjamin, T. B. 1981 Steady flows drawn from a stably stratified reservoir. *J. Fluid Mech.* **106**, 245–260.

Dalziel, S. B. 1992 Maximal exchange in channels with nonrectangular cross sections. *J. Phys. Oceanogr.* **22**, 1188–1206.

Engqvist, A. 1996 Self-similar multi-layer exchange flow through a contraction. *J. Fluid Mech.* **328**, 49–66.

Engqvist, A. & Stenström, P. 2004 Archipelago strait exchange processes – an overview. *Deep-Sea Res.* (in press).

Hogg, A. M. & Killworth, P. D. 2004 Continuously stratified exchange flow through a contraction in a channel. *J. Fluid Mech.* **499**, 257–276.

Killworth, P. D. 1992 On hydraulic control in a stratified fluid. *J. Fluid Mech.* **237**, 605–626.

Lane-Serff, G. F., Smeed, D. A. & Postlethwaite, C. R. 2000 Multi-layer hydraulic exchange flows. *J. Fluid Mech.* **416**, 269–296.

Marshall, J., Adcroft, A., Hill, C., Perelman, L. & Heisey, C. 1997 A finite-volume, incompressible Navier Stokes model for studies of the ocean on parallel computers. *J. Geophys. Res.* **102**, 5753–5766.

Stenström, P. 2003 Mixing and recirculation in two-layer exchange flows. *J. Geophys. Res.* **108**, 10.1029/2002JC001696.

Wood, I. R. 1968 Selective withdrawal from a stably stratified fluid. *J. Fluid Mech.* **32**, 209–223.

Zhu, Z. & Lawrence, G. A. 1998 Non-hydrostatic effects in layered shallow water flows. *J. Fluid Mech.* **355**, 1–16.